Soft Matter

PAPER

View Article Online
View Journal | View Issue

Cite this: *Soft Matter*, 2016, 12, 8690

Determination of physical emulsion stabilization mechanisms of wood hemicelluloses *via* rheological and interfacial characterization

K. S. Mikkonen,*[a] D. Merger,[b] P. Kilpeläinen,[c] L. Murtomäki,[d] U. S. Schmidt[e] and M. Wilhelm[b]

Received 7th July 2016,
Accepted 19th September 2016

DOI: 10.1039/c6sm01557c

www.rsc.org/softmatter

Materials manufacturing industries seek efficient, economic, and sustainable compounds for stabilizing dispersed systems such as emulsions. In this study, novel, abundant biobased hydrocolloids spruce galactoglucomannans (GGM) and birch glucuronoxylans (GX) were obtained from a forestry biorefining process and characterized as versatile stabilizers of rapeseed oil-in-water emulsions. For the first time, GGM and GX isolated by pressurized hot water extraction (PHWE) of spruce and birch saw meal, respectively, were studied in emulsions. The PHWE wood hemicelluloses—polysaccharides with relatively low molar mass—facilitated the formation of emulsions with small average droplet size and efficiently prevented droplet coalescence. GGM and GX lowered the surface tension of emulsions' oil–water interface and increased the viscosity of the continuous phase. However, viscosity of the wood hemicellulose-based systems was low compared to that of commercial polymeric stabilizers. GGM-stabilized emulsions with varying oil volume fractions were characterized in terms of their rheological properties, including large amplitude oscillation shear (LAOS) measurements, and compared to emulsions prepared with a classical small-molecular surfactant, Tween20. The physical emulsion stabilization mechanisms of GGM and GX are suggested as steric repulsion assisted by Pickering-type stabilization. Wood hemicelluloses have potential as highly promising future bioproducts for versatile industrial applications involving colloidal systems and soft materials.

Introduction

Emulsions are colloidal dispersions formed by two immiscible liquids.[1] The dispersed phase of an emulsion appears as droplets of a certain size distribution immersed in the continuous phase of another liquid. The properties of emulsions—appearance, rheology, and physical stability—may follow those of the constituents or show completely new material behavior based on the spatial distribution and interactions of polymers, particles, and droplets.[2] The most abundantly used emulsions are those consisting of oil and an aqueous phase, that is, oil-in-water (o/w) or water-in-oil (w/o) emulsions.[1] They are used in the chemical industry, pharmaceuticals, cosmetics, and food, the latter of which can be viewed as a "complex form of soft matter".[2] Food emulsions include creams, spreads, dressings, and beverages. Thus, emulsions are versatile systems with wide industrial applications and multiple functions.

Owing to the immiscible nature of the dispersed and the continuous phases, emulsions are thermodynamically unstable systems that tend to minimize their interfacial area, leading to structural breakdown during storage. Emulsion breakdown can be slowed down remarkably by using emulsifiers and stabilizers to ensure emulsion-structured materials have a reasonable shelf life. Commonly used emulsifiers include amphiphilic, surface-active molecules such as phospholipids, sodium dodecyl sulphate, and polysorbates (*e.g.*, Tween20). Many food materials also exploit the capacity of proteins and certain polysaccharides to stabilize emulsions.[2] We recently characterized novel, highly abundant, but unexploited forestry biorefinery products, namely, spruce galactoglucomannans (GGM), as efficient natural stabilizers of rapeseed oil-in-water emulsions.[3,4] GGM belong to a diverse group of hemicelluloses: non-cellulosic plant cell wall polysaccharides closely associated with cellulose and lignin.[5] Wood contains 25–35 wt% hemicelluloses, and GGM can be recovered from industrial softwood streams with high yield and purity.[6] Naturally occurring lignin–hemicellulose complexes were considered to introduce

[a] *Department of Food and Environmental Sciences, 00014 University of Helsinki, P. O. Box 27, Finland. E-mail: kirsi.s.mikkonen@helsinki.fi*
[b] *Institute for Chemical Technology and Polymer Chemistry, Karlsruhe Institute of Technology, Germany*
[c] *Natural Resources Institute Finland, Viikinkaari 4, 00790 Helsinki, Finland*
[d] *Department of Chemistry, Aalto University, P. O. Box 16100, 00076 Aalto, Finland*
[e] *Institute of Process Engineering in Life Sciences, Section I: Food Process Engineering, Karlsruhe Institute of Technology, Germany*

functionality to GGM and be responsible for their capacity to greatly enhance both the physical[3] and oxidative[4] stability of emulsions. GGM have potential as a multifunctional, sustainable, and economic alternative to existing hydrocolloids. Xylans, the major hemicelluloses in hardwoods, are another type of industrially significant, but underutilized biorefinery streams that could be used as biobased materials or hydrocolloids.[7]

To efficiently apply hemicelluloses as stabilizers in novel formulations, their function mechanisms such as the interaction between emulsion droplets containing adsorbed hemicelluloses and their effects on emulsion stability must be understood. Analysis of emulsions' viscoelastic properties as a function of the dispersed phase volume fraction is a powerful tool for studying such phenomena.[8] Most rheological models of dilute emulsions are based on ellipsoidal deformation models, in which the morphology of the dispersed phase is assumed to be globular, and a single droplet is modeled as an ellipsoid under deformation.[9] The relevant parameters include viscosities of the dispersed and the continuous phases, interfacial tension between the phases, radius of undistorted spherical droplets, and maximum shear rate of macroscopic flow.[9] Industrial emulsions are often exposed to strong external shear, resulting in large interface deformations far beyond the linear viscoelastic regime.[10] In addition to conventional oscillatory shear studies conducted at small amplitudes, the non-linear regime can be characterized using large amplitude oscillatory shear (LAOS) flow, that is, Fourier transform rheology (FTR), to mimic a variety of technical conditions and to distinguish even small differences between dispersions.[11] LAOS experiments can relate nonlinear rheological properties to droplet size and droplet size distribution of emulsions and, thus, provide useful insight into their stability.[12] In the present study, the authors aimed to characterize the rheological and interfacial properties of hemicellulose-stabilized emulsions at varying volume fractions in order to explain the function mechanisms and assess the industrial application potential of wood hemicelluloses in novel soft matter constructions.

Results and discussion

Emulsion preparation with PHWE hemicelluloses

We extracted hemicelluloses from spruce and birch saw meal by using the pressurized hot water extraction (PHWE) method.[7] PHWE is considered a green and clean wood fractionation method that uses water without added chemicals and produces hemicelluloses that are hypothesized to be safe for food contact and oral intake. The carbohydrate composition of the ethanol precipitated extracts was similar to those studied previously.[7] In addition to carbohydrates, the GGM and glucuronoxylan (GX) preparations contain phenolic compounds, part of which are assumed to remain in the samples after ethanol precipitation.[4,7]

The average molar mass of GGM was 10 000 g mol^{-1} and that of GX was 6500 g mol^{-1}. Compared to some other polysaccharides, for example, cellulose or starch, the molar masses of PHWE wood hemicelluloses are low. That restricts their use in some material applications such as packaging films, where mechanical strength is needed. Previously, we prepared emulsions[3] using GGM from spruce thermomechanical pulping (TMP) process water, which had a slightly higher molar mass of about 20 000–40 000 g mol^{-1}.[3,13,14] We showed that the fraction of GGM adsorbed on the oil–water interface consisted of larger molecules than the fraction remaining in the continuous aqueous phase of an emulsion. Our present results show that despite their lower molar masses, PHWE hemicelluloses functioned as efficient emulsifiers. It should be pointed out here that determination of the molar mass of polysaccharides with high accuracy is very challenging, as discussed by Maina *et al.*[15] Thus, we suggest that the molar mass values be considered rough indications of polysaccharide size and not as exact values.

In an earlier work,[3] we efficiently stabilized rapeseed oil-in-water emulsions by using up to 1 wt% TMP GGM and up to 5 wt% oil, as indicated by the small droplet size maintained during four weeks of storage. In the present study, we tested emulsions with higher GGM and oil contents than before, while maintaining a constant GGM : oil ratio during emulsion preparation (Table 1). Emulsification was successful with all tested GGM and oil contents, and the resulting emulsions had a white, milky sample appearance, indicating the formation of small oil droplets.[16]

For the first time, PHWE birch GX was tested as an alternative wood-based stabilizer and was compared to GGM. The appearance of GX25 emulsions was similarly white, opaque and milky as that of GGM emulsions. The emulsifying properties of hemicelluloses were compared to those of the classical surfactant emulsifier Tween20, a food grade compound. Furthermore, dairy cream was tested to compare the properties of hemicellulose

Table 1 Emulsion codes, constituents, oil volume fractions, and preparation methods. The emulsifier : oil ratio was 1 : 5

Sample code	Emulsifier (wt%)	Rapeseed oil (wt%)	Oil volume fraction	Preparation method
GGM5	Galactoglucomannan 1	5	0.059	UT 5 min at 9800 rpm + MF
GGM20	Galactoglucomannan 4	20	0.23	UT 5 min at 9800 rpm + MF
GGM25	Galactoglucomannan 5	25	0.29	UT 5 min at 9800 rpm + MF
GGM40	Galactoglucomannan 8	40	0.47	UT 5 min at 9800 rpm
GGM60	Galactoglucomannan 12	60	0.70	UT 3 min at 10 000 rpm
GX5	Glucuronoxylan 1	5	0.059	UT 5 min at 11 000 rpm + MF
GX25	Glucuronoxylan 5	25	0.29	UT 5 min at 9800 rpm + MF
T40	Tween20 8	40	0.47	UT 7 min at 10 000–18 000 rpm
T60	Tween20 12	60	0.70	UT 3 min at 10 000 rpm

UT = Ultra-Turrax, MF = Microfluidizer.

emulsions to those of an existing industrial product. The purpose was to highlight the potential application of hemicelluloses in food products. Finally, spruce GGM-stabilized emulsions were selected for detailed characterization by varying oil volume fractions based on evidence of GGM's promising emulsifying and stabilizing capacity obtained in our previous studies.[3,4]

Droplet size distributions and interfacial tension

Droplet size distribution analysis of freshly prepared emulsions confirmed that all studied hemicellulose–oil systems contained fine droplets (Fig. 1). The D[3,2] average droplet size of fresh GGM5 emulsion was 0.43 μm, which agrees with that of TMP GGM emulsions studied previously at a similar GGM : oil ratio (Table 3).[3] The droplet size distributions visualized a major population of oil droplets measuring approximately 0.3 μm and a second population of droplets measuring approximately 1.2 μm. The second peak was most likely partially composed of flocculated droplets, as shown previously for GGM emulsions.[3]

The average droplet size of the fresh GGM20 and GGM25 emulsions was similar to that of GGM5 emulsions (Table 2). The fresh GGM20 and GGM25 emulsions only showed one peak, but a second peak appeared after storage for one month (Fig. 1). The GGM40 and GGM60 emulsions exhibited small D[3,2] average droplet sizes of approximately 9 and 2 μm, respectively, even though emulsification was achieved only through mechanical stirring using a mixer (Tables 1 and 2). The GGM40 and GGM60 emulsions contained only a single distribution of droplets, which was maintained during storage

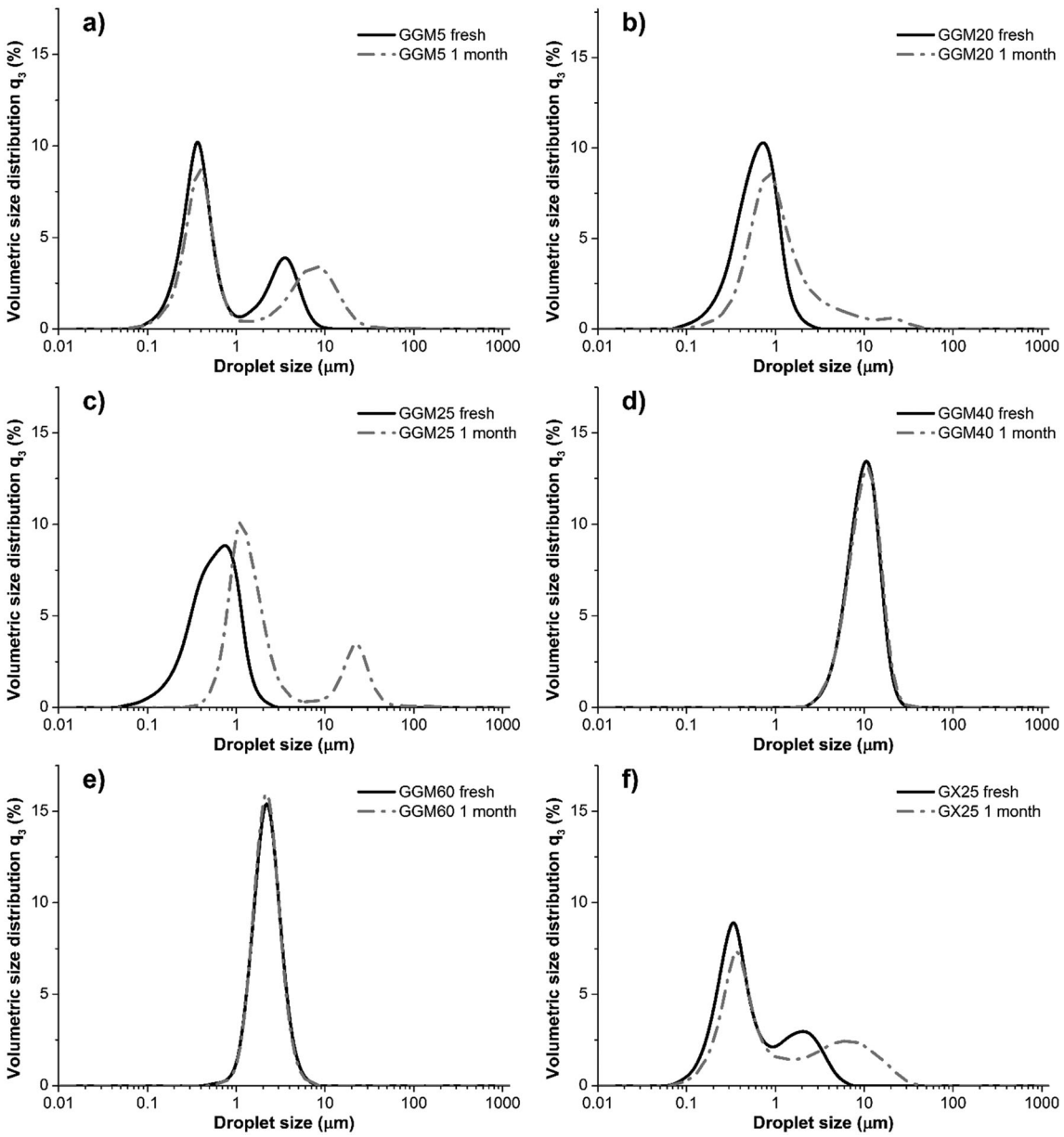

Fig. 1 Droplet size distributions of emulsions as fresh and after one month storage at RT. The sample codes are explained in Table 1.

Table 2 Average droplet size D[3,2] of fresh emulsions and those stored for one month at RT. The sample codes are explained in Table 1

	Average droplet size D[3,2] (μm)	
Sample	Fresh emulsions	Emulsions stored for one month at RT
GGM5	0.43	0.52
GGM20	0.50	0.82
GGM25	0.43	1.5
GGM40	8.7	8.8
GGM60	2.1	2.1
GX25	0.39	0.53
T40	5.1	n.d.
T60	2.0	n.d.

n.d. = not determined.

for one month at RT (Fig. 1). The GX25 emulsions were similar to the GGM25 emulsions with respect to droplet size distribution. This shows that the novel birch hemicelluloses are suitable for stabilizing the same small droplet sizes as spruce hemicelluloses.

The GX and GGM emulsions, except GGM40, maintained their opaque milky appearance over several months of storage at RT. In contrast, GGM40 separated into a creamed layer and an aqueous solution within approximately one week. The GGM40 layers could be remixed by turning the emulsion container upside down, after which the dispersion again slowly separated into creamed and solution layers within about a week. The fresh Tween20-stabilized T40 and T60 emulsions had a milky appearance similar to the GGM and GX emulsions, but the former creamed faster, showing visual separation within a few days. According to Stokes' law (eqn (1)), where R is the droplet radius, $\Delta\rho$ is the density difference between the two components, g is the gravitational constant, and η_s is the continuous phase viscosity; the creaming rate v_{cr} of an emulsion is proportional to R^2. Therefore, the creaming of the GGM40, T40, and T60 emulsions can be explained partially by their larger droplet size in comparison with the other studied emulsions.

$$v_{cr} = \frac{2R^2\Delta\rho g}{9\eta_s} \quad (1)$$

The efficient emulsification and stabilization capacity of GGM was previously hypothesized to be due to GGM's tendency to form intra- and intermolecular assemblies, that is, aggregates in aqueous system[4,17] that may induce the so-called Pickering stabilization by particles.[18] In addition, GGM is associated with wood-derived phenolic residues that most likely contribute to emulsion stabilization by introducing an amphiphilic character to GGM.[4] In the present work, we characterized the interfacial tension of the GGM and GX solutions against rapeseed oil to further understand the stabilization mechanisms. Rapeseed oil naturally contains antioxidants and other impurities that may contribute to its behavior at the aqueous interface; this was illustrated by the low surface tension (9.2 mN m^{-1}) of the sodium citrate buffer solution against oil. The continuous phases of the GGM5, GGM25, and GX25 emulsions showed slightly lower surface tension values of 8.8, 8.2, and 8.8 mN m^{-1}, respectively. The surface activity of wood hemicelluloses was not comparable to that of Tween20, whose solution dispersed immediately in oil after injection, because of which surface tension could not be measured. However, even the small detected decrease in surface tension owing to the presence GGM and GX in aqueous solutions may be highly significant in emulsification, given the large total surface area between the oil droplets and the continuous phase of emulsions.

Solution viscosity

Solutions of GGM and GX, representing the continuous phases of emulsions, showed very low viscosity (Table 3) and Newtonian behavior, even for GGM contents of up to 30 wt%. The increase in viscosity owing to GGM is plotted in Fig. 2 as specific viscosity $\eta_{sp} = \frac{\eta_0}{\eta_s} - 1$ depending on the coil overlap parameter $c[\eta]$,[19] where η_0 is the solution viscosity, η_s is the

Table 3 Viscosity of GGM and GX emulsions as fresh and after one month storage at room temperature (RT), as well as that of fresh emulsion constituents and reference samples: cream and Tween20. The sample codes are explained in Table 1

	Viscosity (mPa s) at 100 l s^{-1}		
Sample	Continuous phase	Fresh emulsions	Emulsions stored for one month at RT
GGM5	1.0	1.1	1.2
GGM20	1.9	4.1	3.9
GGM25	2.5	6.5	6.3
GGM40	6.9	43.1	47.5
GGM60	71	2925	3840
GX25	2.0	4.5	4.4
T40	2.0	16.5	149
T60	14.7	324	377
Rapeseed oil	58	n.a.	n.a
Buffer solution	0.7	n.a.	n.a
Cream 12% fat	n.d.	5.9	n.d
Cream 25% fat	n.d.	37	n.d.

n.a. = not applicable, n.d. = not determined.

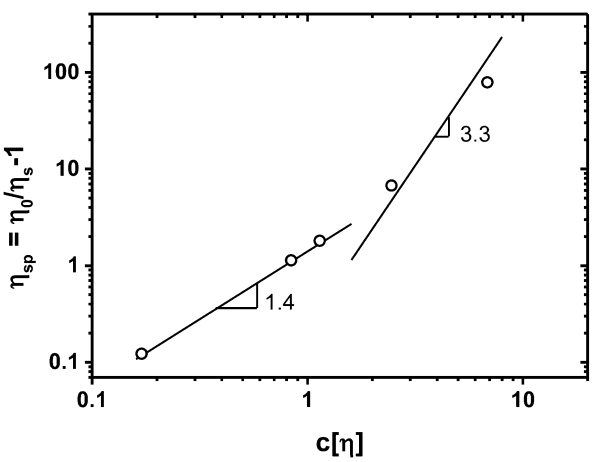

Fig. 2 Specific viscosity of aqueous galactoglucomannan (GGM) solutions as a function of coil overlap parameter $c[\eta]$;[19] concentrations c are 0.011, 0.052, 0.071, 0.153 and 0.427 g ml^{-1}, $[\eta]$ = 16 ml g^{-1}. The lines represent power laws with the indicated exponents.

viscosity of the suspending medium, in this case, water, $[\eta]$ = 16 ml g^{-1} is the intrinsic viscosity of GGM, as determined by size exclusion chromatography, and c is the concentration of GGM. For low GGM contents, the increase in viscosity followed a power law with an index of 1.4, consistent with[20] various polysaccharides including dextran, guar gum, and lambda carrageenan. This is the dilute regime, where individual coils do not overlap. The transition from the dilute to the concentrated regime for the polysaccharides studied previously[20] occurred at $c[\eta]$ values close to 4. Our data are consistent with this, as the two higher concentrations corresponded to higher viscosities than expected from the dilute power law index of 1.4. Exact determination of the power law index for the concentrated regime in our system, however, requires more data. The increase in viscosity was also very low in comparison to that observed for solutions of TMP GGM with higher molar mass (20 000–40 000 g mol^{-1}), studied by Xu *et al.*[13,21] They observed shear thinning behavior for GGM contents higher than 5 wt%. The present solutions of PHWE GGM displayed viscosities that were 7–10 times higher than the respective solutions of Tween20 of the same weight percentage, which is due to the polymeric nature of GGM (Table 3). Thus, the viscosity effect of PHWE GGM as stabilizer is intermediate to those of small-molecular-weight surfactants and high-molar-mass polymers.

Emulsion viscosity

The viscosities of both emulsions and continuous phases at 100 s^{-1} are summarized in Table 3. Furthermore, Fig. 3 shows the shear-rate-dependent viscosity of selected emulsions after 1 month of storage. The GGM emulsions containing lower oil volume fractions of 0.059 (GGM5), 0.234 (GGM20), 0.29 (GGM25), and 0.47 (GGM40) showed Newtonian behavior even after 1 month of storage (data not shown except for GGM40, see Fig. 3). Only the GGM60 emulsion with the highest studied volume fraction (ϕ = 0.70) displayed shear thinning behavior. By contrast, Tween20-stabilized emulsions showed shear thinning behavior at lower volume fractions (T40 and T60). Dickinson *et al.*[22] measured the viscosity of Tween20-stabilized emulsions of mineral oil in water and observed that emulsions containing 30 and 40 wt% oil showed Newtonian behavior, while those containing >50 wt% oil exhibited shear thinning. For Tween20-stabilized emulsions at ϕ = 0.5, a relative viscosity of approximately 10 was reported,[22] which is consistent with our present data. As the emulsions with the highest studied volume fractions showed the most interesting rheological response, the following discussion is focused mainly on comparing the GGM40, GGM60, T40, and T60 emulsions.

The shear thinning behavior of the GGM60 emulsion was less pronounced (η decreased as $\dot{\gamma}^{-0.22}$ for shear rates between 10^{-2} and 10 s^{-1}) than that of the T40 ($\eta \propto \dot{\gamma}^{-0.69}$) and the T60 emulsions ($\eta \propto \dot{\gamma}^{-0.66}$). This was ascribed to the higher viscosity of the continuous phase of the GGM60 emulsion due to the polymeric nature of GGM. As the oil volume fraction of the Tween20-stabilized emulsions increased, shear thinning became more pronounced, which is consistent with previously obtained results for emulsions stabilized by ionic[23] or non-ionic surfactants.[24]

The relative viscosities $\eta_r = \eta/\eta_s$ of the emulsions as a function of volume fraction are shown in Fig. 4 (for emulsions, the solution viscosities from Table 2 are taken as η_s). The results are consistent with hard sphere dispersion behavior, as described by the model of Krieger and Dougherty,[25] eqn (2). The maximum packing fraction ϕ_{max} in eqn (2) ranges from 0.64 for random close packing of monodisperse spherical particles to 0.74 for hexagonal packing. For random packing, polydispersity and particle softness usually allow for maximum packing fractions larger than 0.64.[23] If we consider the low-shear-rate viscosities, we find that ϕ_{max} = 0.71 best describes the data.

$$\eta_r = \frac{\eta}{\eta} = \left(1 - \frac{\phi}{\phi_{max}}\right)^{-2.5\phi_{max}} \quad (2)$$

In Fig. 4, we also show the emulsion viscosities at $\dot{\gamma}$ = 100^{-1}, which were significantly lower than those at $\dot{\gamma}$ = 0.01 s^{-1} owing

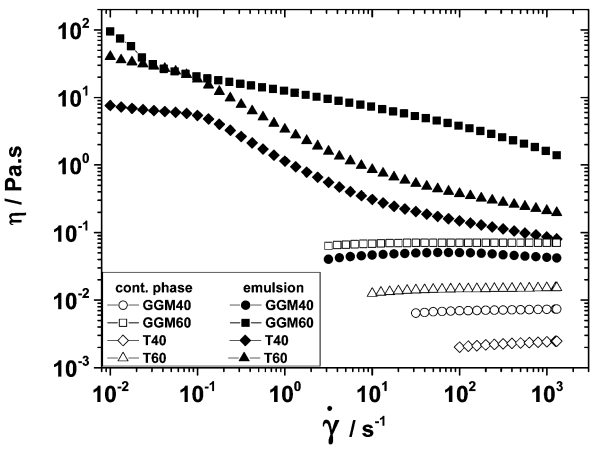

Fig. 3 Shear-rate-dependent viscosity of high volume fraction emulsions stabilized with galactoglucomannan (GGM) and Tween20 (T) and the respective continuous phases at 25 °C after 1 month of storage. The numbers indicate oil fraction in wt%.

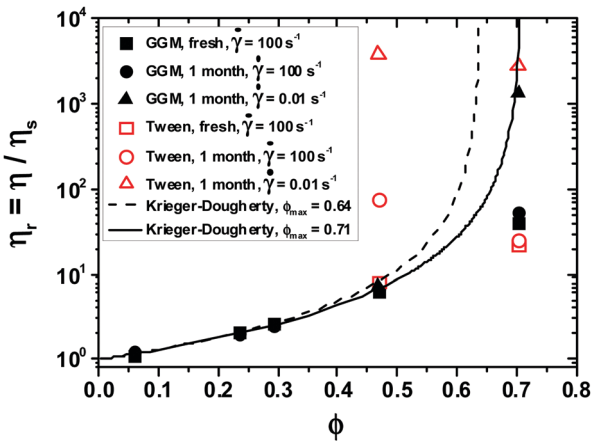

Fig. 4 Relative viscosities of galactoglucomannan (GGM) (closed symbols) and Tween20 (open symbols)-stabilized emulsions as a function of volume fraction at T = 25 °C.

to shear thinning. At higher shear rates, ϕ_{max} increased owing to ordering of the previously random structure. De Kruif *et al.*[19] investigated the dependence of ϕ_{max} on shear rate in a sterically stabilized suspension. For $\dot{\gamma} \rightarrow \infty$, the authors reported $\phi_{max} = 0.70 \pm 0.02$. In our measurements, higher values of ϕ_{max} for high-shear-rate viscosity were obtained because liquid oil droplet deformation leads to the formation of a more compact structure than do solid suspension particles.

In contrast to hard sphere or sterically stabilized dispersions, electrostatically stabilized systems exhibit much higher viscosities.[22] In such systems, viscosity diverges at a lower volume fraction[26] than in nonionic systems, because the electrostatic interaction provides an additional contribution to the viscosity, and the electrostatic double layer increases the effective volume fraction. Because the absolute value of the GGM emulsions' ζ potential (≈ -10 mV)[3] is low and the viscosities of the GGM emulsions follow the Krieger–Dougherty model, potential electrostatic effects seemed to be negligible in this system, which supports the idea that GGM stabilize oil droplets by a sterical effect. On the other hand, the GX emulsion's ζ potential was -35 mV, which is presumably due to the anionic methyl glucuronic acid and galacturonic acid residues in GX. The anionic surface charge may contribute to GX's stabilizing capacity. The role of electrostatic effects on GX emulsions' viscosity as the function of oil volume fraction will be a subject of further studies.

The emulsions' viscosity did not change significantly after one month of storage (compare rectangular and circular symbols in Fig. 4). An exception was the T40 sample, which had an exceptionally high viscosity after one month of storage (Fig. 3). This could be attributed to differences in oxidation of the emulsions' lipid phase, that is, rapeseed oil, and the resulting changes in component interactions. Our previous work showed that GGM efficiently inhibits lipid oxidation,[4] whereas Tween20 is not expected to inhibit oxidation.

Tween20 is a classical small-molecular-mass surfactant, and it is an efficient emulsifier. However, creaming and phase separation of the T40 and the T60 emulsions were visually noted after storage for a few days. By contrast, GGM acted both as an emulsifier and a stabilizer that increased the emulsion's shelf life. This correlates with the higher viscosity of the GGM40 and the GGM60 emulsions compared to the corresponding T40 and T60 emulsions. A potential future product of GGM could be a vegetable oil-based replacement for dairy cream. To compare the GGM-stabilized emulsion systems with industrial food emulsions, the viscosity of dairy cream samples with 12 and 25 wt% fat was measured at $\dot{\gamma} = 100^{-1}$ (Table 3). The dairy cream samples showed higher viscosity than the GGM-rapeseed oil emulsions at similar or slightly higher fat contents.

GGM-stabilized emulsions have potential for application in the food, cosmetics, pharmaceutics, paint, and coating industries. The intermediate viscosity of GGM solutions and emulsions indicates that GGM facilitates the formation of materials with a wide range of flow properties. GGM acts as an emulsifier, allowing for the formation of relatively low-viscosity emulsions, and stabilizer, extending the physical stability of such emulsions. If higher viscosity is desired, it can be achieved by adding a texture modifier such as a polysaccharide with a higher molar mass. Furthermore, the Newtonian behavior of GGM solutions and emulsions at low to intermediate oil volume fractions indicates that GGM-based soft materials would be easy and predictable to process with industrial equipment.

Linear viscoelastic moduli

As the emulsions with the highest studied volume fractions showed the most interesting phenomena so far, the corresponding samples were subjected to oscillatory rheological measurements as well. The trends that were found for steady shear viscosity are also evident in the frequency-dependent moduli shown in Fig. 5 for the GGM40, GGM60, T40, and T60 emulsions. The GGM40 emulsion was essentially a liquid, as the loss modulus G'' dominated the entire measured frequency range, and measurable values of the storage modulus G' occurred only above 70 rad s^{-1}. The GGM60, T40 and T60 emulsions displayed viscoelastic behavior. The two Tween20-stabilized emulsions T40 and T60 showed crossover from viscous behavior at low frequencies to predominantly elastic behavior at higher frequencies, as expected. The cross-over frequency ω shifted downward (15.49 rad s^{-1} to 4.7 rad s^{-1}) when ϕ was increased from 0.47 to 0.7, which is qualitatively consistent with previous data on poly(vinylalcohol)-stabilized oil-in-water emulsions[8] and polydimethylsiloxane-in-water emulsions stabilized by sodium dodecyl sulphate,[27] for example. Note that in the case of electrostatic stabilization,[27] elastic contributions were significantly higher, as evidenced by the domination of G' over G'' in a frequency window of three decades at volume fractions as low as 0.57. Notably, the viscoelastic properties of GGM60 were dominated by the viscosity of the continuous phase ($G'' > G'$), although the effect of increased droplet interaction was evident in the appreciable elasticity detected by G'. However, we did not find a crossover to an elastically dominated regime with increasing ω. Thus, the viscoelastic behavior of the GGM40 and the GGM60 emulsions differed qualitatively from the properties of oil-in-water emulsions stabilized by non-ionic surfactants.[24] Again, this is related to the high viscosity of the continuous phase which, for GGM60, surpasses the oil viscosity (see Table 3). Therefore, the elasticity arising from particle interaction and crowding is far less pronounced in the viscoelastic spectra.

Large amplitude oscillatory shear results

Nonlinear viscoelastic properties of complex matter can be probed conveniently by large amplitude oscillatory shear (LAOS) experiments, where in an oscillatory shear test, strain amplitude which is beyond the linear viscoelastic regime of the studied material is applied.[11,28,29] When studying solid-like viscoelastic materials such as concentrated suspensions, emulsions, and gels, increasing the strain amplitude γ_0 in discrete steps leads to a transition from predominantly solid ($G' > G''$) to liquid ($G'' > G'$) behavior, which is termed yielding. An early study of the yielding behavior of emulsions using LAOS was conducted.[27] In this work, the strain amplitude at which yielding occurred, or yield strain, was reported to vary between 0.048 and 0.15 with increasing volume fraction, with a local minimum at $\phi = 0.63$. The corresponding yield

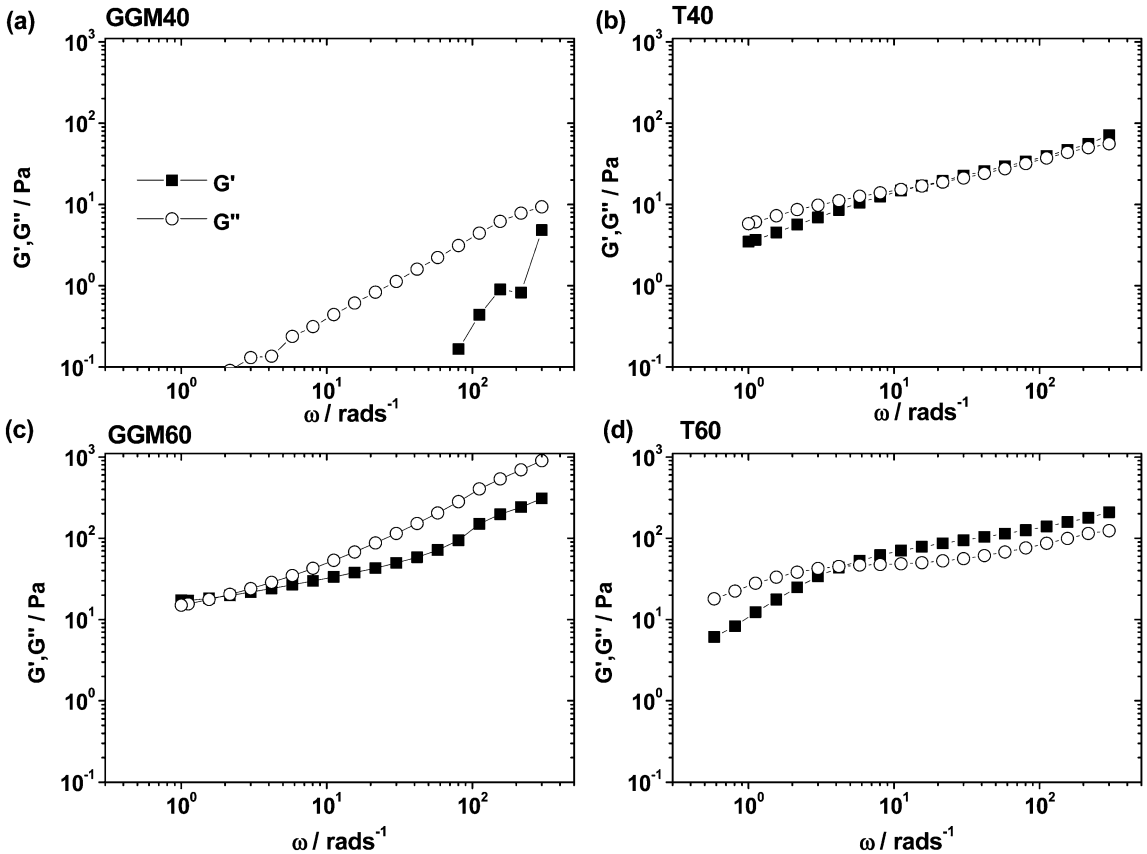

Fig. 5 Linear viscoelastic moduli of galactoglucomannan (GGM)- and Tween20 (T)-stabilized emulsions containing oil volume fractions of 0.47 (GGM40 and T40) and 0.7 (GGM60 and T60), as measured at γ_0 = 0.01 and T = 25 °C.

stress increased proportionally to the distance from the random packing volume fraction $(\phi - 0.62)^2$. Other authors have investigated the influence of the elasticity of the dispersed phase on yielding behaviour[30] and employed rheo-imaging to investigate the yielding of particle-stabilized (Pickering) emulsions with adjustable interactions between droplets.[31] Oil-in-water emulsions with volume fractions ranging from 0.79 to 0.94 were considered by Pal.[32] Pal determined yield stress and storage modulus by steady shear, oscillatory shear, and creep/recovery measurements and compared the results to predictions obtained using the Princen and Kiss theory.[33] To gain insight into the nonlinear viscoelastic properties of GGM-stabilized emulsions, we conducted LAOS experiments on the GGM40, GGM60, T40, and T60 samples containing 40 and 60 wt% oil, corresponding to volume fractions of 0.47 and 0.7, at angular frequencies of 1 rad s^{-1} and 20 rad s^{-1} (Fig. 6). The GGM40 emulsion showed dominating viscous behavior at all strain amplitudes γ_0. For larger values of γ_0, finite values of the storage modulus G' became measurable, signifying the elastic process of droplet collision, which was more pronounced at higher frequencies owing to higher shear rate amplitudes ($\dot{\gamma}_0 = \omega\gamma_0$). For $\gamma_0 > 1$, a mild increase in the loss modulus was observed for the GGM40 emulsion, and this loss was more pronounced for the GGM60 emulsion. This feature might be interpreted as shear thickening behavior, which is commonly observed in particle dispersions.[34–36] Shear thickening is believed to be caused by the formation of large particle clusters at high shear rates, whereby the rheology is dominated by lubrication hydrodynamics.[26] In emulsions, shear thickening is rare, but it has been observed in oil-in-water emulsions stabilized by adsorbed colloidal silica.[37] In the present reference samples, where droplet stabilization was achieved by Tween20 (T40 and T60 emulsions), shear thickening was not observed. That we found shear thickening in GGM-stabilized emulsions suggests that the stabilization mechanism involves adsorption of solid GGM particles on the oil–water interface (Pickering-type stabilization). Hermes and Clegg[31] reported shear thickening in the LAOS flow of a Pickering emulsion, which was accompanied by droplet cluster formation, as visualized by confocal microscopy imaging. The absence of shear thickening in steady shear flow of our GGM emulsions, however, contradicts this argument. An alternative explanation for the local increase in G'' might be the so-called Payne effect, which has been observed for emulsions[27] and a variety of other particulate systems such as filled elastomers,[38] glassy suspensions,[39] colloidal gels,[40] and foams.[41] The common interpretation of the Payne effect is increased dissipation owing to breakage of the network or cage structure in the suspension case. In all these cases, the initial material response in the linear viscoelastic regime was dominated by elasticity ($G' > G''$), and the storage modulus G' and the magnitude of the complex modulus $|G^*|$ decreased with

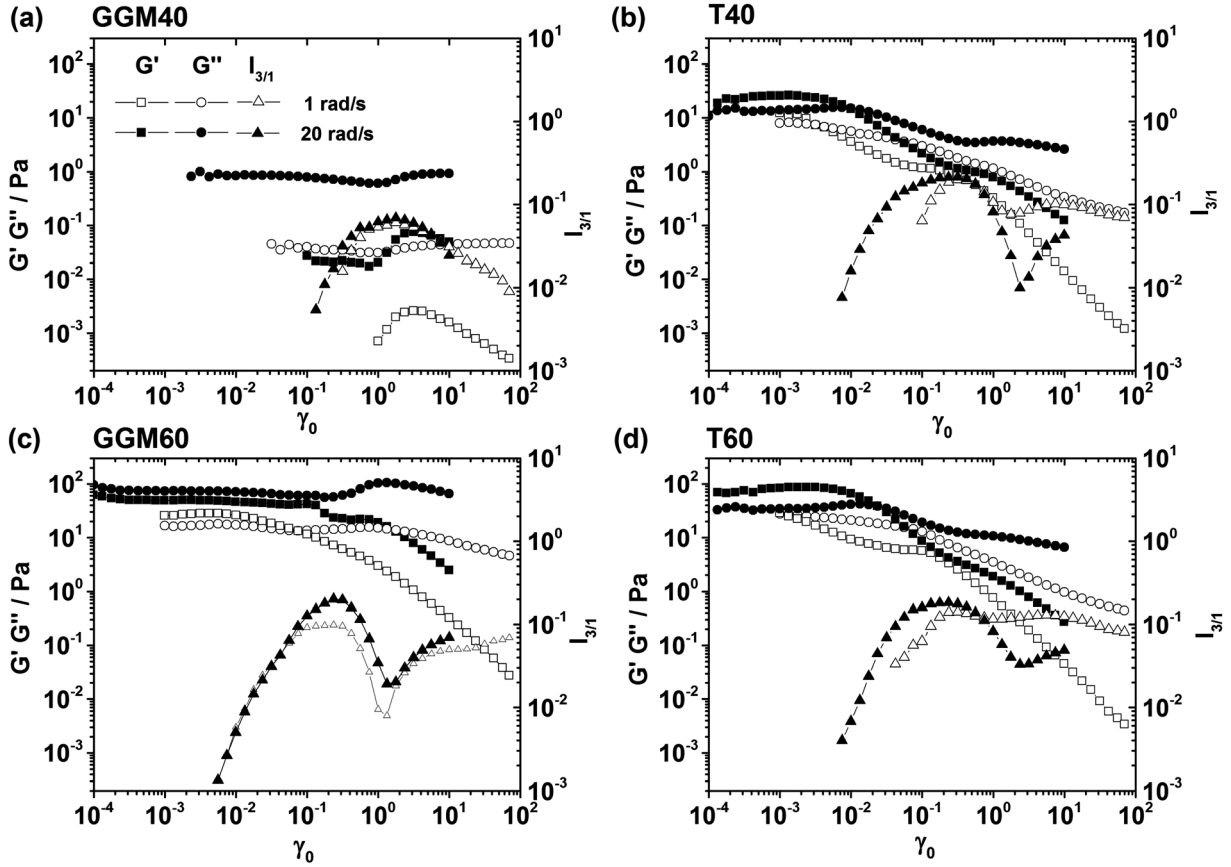

Fig. 6 Large amplitude oscillatory shear results (storage modulus G', loss modulus G'', and normalized third harmonic intensity $I_{3/1}$) of galactoglucomannan (GGM)- and Tween20 (T)-stabilized emulsions containing oil volume fractions of 0.47 (GGM40 and T40) and 0.7 (GGM60 and T60) at angular frequencies of 1 rad s^{-1} (open symbols) and 20 rad s^{-1} (closed symbols); T = 25 °C.

increasing strain amplitude. By contrast, for the GGM emulsions presented in this work, viscous behavior dominated ($G'' > G'$) at small amplitudes and ω = 20 rad s^{-1}, and $|G^*|$ displayed a local maximum as well. Additionally, recent model calculations made using a modified Maxwell model, which incorporated shear thinning viscosity,[42] revealed that the Payne effect does not necessarily requires a microscopic bond breaking mechanism, and it can result from a combination of shear thinning and elasticity-dominated behavior at high frequencies. Thus, we conclude that this effect in our samples was indeed shear thickening, and it must be distinguished from the Payne effect.

In addition to $G'(\gamma_0)$ and $G''(\gamma_0)$, the relative intensity of the third harmonic (normalized to the fundamental frequency intensity), $I_{3/1}$, was shown as a measure of the stress waveform's deviation from the pure sinusoidal reference.[11,29] Judging by the γ_0-dependent storage and loss moduli of the GGM60 emulsion, the linear range at 20 rad s^{-1} extended up to γ_0 = 0.2, whereas at 1 rad s^{-1}, deviations in G' occurred at γ_0 = 0.01. An inspection of $I_{3/1}$, however, revealed similar levels of waveform distortion, as $I_{3/1}$ became measurable at $\gamma_0 \sim 0.006$ at both frequencies. For the GGM60, T40, and T60 emulsions, $I_{3/1}$ showed an initial increase, a local maximum, followed by a local minimum, and further increase with increasing γ_0. This suggests that the evolution from linear to nonlinear response involved a two-step process. Two-step or multi step-yielding of colloidal yield stress fluids has been studied using several colloidal gels.[40,43,44] The first yielding is associated with the breaking of network strands of the gel structure, whereas the second yielding is thought to be a signature of the breaking of particle clusters into individual particles. Based on the data of Mason *et al.*[27] and Pal,[32] a two-step process was not expected for our emulsion system. The details of the underlying processes should be explored in future by employing complementary optical or scattering methods to assess microstructure during flow.

Although at 20 rad s^{-1}, the response of the GGM60 emulsion was predominantly viscous, G'' dominated G' at all strain amplitudes in the case of the T40 and the T60 emulsions, and classical yielding behavior was observed, that is, initially $G' > G''$, followed by crossover of the moduli (Fig. 6b and d). Using flow visualization with a confocal microscope and by comparing photographs of the same phase of an oscillation, Hermes and Clegg[31] reported a decorrelation of the emulsion structure in the vicinity of the $G' - G''$ crossover. This decorrelation signifies cage breaking, which results in increased droplet mobility and irreversible changes in the arrested emulsion structure. For the 20 rad s^{-1} experiments, we found that the crossover of G' and G'' occurred at a critical γ_0, which increased from 0.0086 to 0.0236 when ϕ was increased from 0.47 to 0.7

(Fig. 6b and d); this can be interpreted as an increase in the structural strength of the emulsion with increasing ϕ.

The main difference between the GGM- and the Tween20-stabilized emulsions was that for the GGM system, viscous behavior dominated at all investigated strain amplitudes; in contrast, the Tween20 system displayed classical yielding behavior. This difference can be related back to the higher viscosity of the GGM-containing solutions used for emulsification.

Emulsion stability assessment from rheological properties

By using rheological results, emulsion stability for a given volume fraction can be predicted based on two effects: increase in the viscosity of the continuous phase or generation of a sample spanning the elastic structure. The creaming rate v_{cr} of an emulsion depends on its viscosity. The upper limit is governed by Stokes' law (eqn (1)) for dilute systems ($\phi < 0.01$).

With increasing ϕ, the creaming velocity decreases to zero at the maximum packing fraction,[45] where the diffusion of droplets is minimized and the emulsion droplet arrangement is arrested. This state is called a glass in analogy to suspensions. A glassy material exhibits a finite yield stress and is predominantly elastic.[46] The higher the yield stress and the elastic modulus, the higher is emulsion stability against creaming. Tadros[45] utilized the criterion $G' > G''$ to classify emulsions as stable because in this case, the arrested structure prevents creaming.

By comparing the viscosities of emulsions and their constituents, we found that the dominant mechanism for the stabilization of the tested GGM emulsions against creaming was the increase in viscosity of the continuous phase. Adding to the stabilizing effect of the arrested structure owing to high volume fraction (GGM60), this resulted in higher creaming stability than that of emulsions stabilized by Tween20. For stabilization against coalescence, the viscous character of the GGM emulsions, as determined by the present rheological investigations, and, especially, the shear thickening observed by LAOS consolidate the hypothesis of a steric mechanism of polymer adsorption at the oil–water interface[3] that also may involve the adsorption of particulate GGM aggregates, which act as Pickering- type stabilizers. Agglomeration of polysaccharides, including hemicelluloses, in aqueous environment is a known phenomenon creditably discussed in *e.g.*, ref. 47, and observed for GGM in ref. 17. Furthermore, from the turbid visual appearance of aqueous GGM and GX solutions, the presence of non-dissolved particles that may function as Pickering-type stabilizers is evident.

Experimental

Materials

Spruce and birch extracts were obtained according to Kilpeläinen *et al.*[7] The extraction of milled spruce saw meal (Metsä Wood sawmill, Renko, Finland) was done at 160 °C for 60 min at flow-through of 20 l min^{-1}. The birch saw meal (Koskisen Oy sawmill, Järvelä, Finland) was extracted at 175 °C for 60 min with a flow-through of 20 l min^{-1}. Fractions were collected and concentrated using a rotary evaporator at 65 °C *in vacuo*. The concentrated spruce extract contained 15% solids, and the birch extract contained 24.4% solids. The extracts were slowly added to ethanol at a concentrate : ethanol ratio of 1 : 8 and then mixed for 10 min. The suspensions were let to stand for 30 min in order to allow the precipitates to sink to the bottom. The samples were filtrated through filtering bags (Eaton NMO-25-P01R-50S, Hyxo Oy, Finland), and solid cakes were collected. The solids were dried in a vacuum oven at 40 °C for two days.

The carbohydrate compositions of the extracted samples were analyzed using gas chromatography (GC) after acid methanolysis by following the method of Sundberg *et al.* (1996).[48] The monosaccharide standards L-arabinose, D-xylose, D-glucose were procured from Merck (Darmstadt, Germany), and D-galactose, D-mannose, L-rhamnose, D-galacturonic acid, and D-glucuronic acid were procured from Fluka and Sigma (St. Louis, MO, USA). Quantification was performed using five concentration levels of each sugar. Methyl glucuronic acid was quantified based on the D-glucuronic acid standard, as described by Chong *et al.*[49] The GC instrument used was an Agilent 6890 N GC system (Agilent Technologies, Foster City, CA, USA) with a flame ionization detector (FID). The system was equipped with an Agilent 7683 series injector and an autosampler that used Agilent ChemStation 06 software for instrument control and data handling. The column used was a DB-1 (30 m, 0.25 mm i.d., 0.25 lm film thickness) by Agilent Technologies. Analysis of the silylated monosaccharides was performed using a gradient system with a total run time of 41.25 min. The initial temperature of 150 °C was held for 3 min, and three linear gradients were followed: (1) 2 °C min^{-1} from 150 to 186 °C, (2) 1 °C min^{-1} from 186 to 200 °C, and (3) 20 °C min^{-1} from 200 to 325 °C. The ethanol-precipitated spruce extract consisted of 53 mol% mannopyranosyl units, 17% xylopyranosyl, 15% glucopyranosyl, 10% galactopyranosyl, and minor fractions of other carbohydrates. The birch extract precipitate consisted of 86 mol% xylopyranosyl units, 4.5% methyl glucuronic acid, 3% glucopyranosyl, 3% mannopyranosyl, 3% galactopyranosyl, and 3% galacturonic acid. Accordingly, the spruce extract was referred to as GGM and the birch extract as GX.

For the molar mass and intrinsic viscosity analysis, GGM and GX were dissolved in dimethyl sulfoxide (DMSO) containing 0.01 M LiBr. The solution was stirred magnetically for three days and then filtered with 0.45 μm syringe filters (GHP Acrodisc 13, Pall Corp., Ann Arbor, MI, USA). The samples were analyzed by high-performance size-exclusion chromatography (HPSEC). The HPSEC analysis equipment was described by Pitkänen *et al.*[50] Pullulans with molar masses of 1320, 11 800, 22 800, 47 300, 112 000, and 212 000 g mol^{-1} were used for column calibration (Postnova Analytics, Landsberg am Lech, Germany).

Rapeseed oil was purchased from a supermarket (Bunge Finland Oy, Raisio, Finland). Ultra-high temperature – treated cream with 12% fat (Friesland Campina Germany GmbH, Heilbronn, Germany) and at least 30% fat (Edeka Zentrale AG & Co, KG, Hamburg, Germany) were also bought from a supermarket. The cream with 30% fat was diluted to 25% fat content with water. Potassium sorbate was procured from BDH Prolabo (VWR International, Darmstadt, Germany), citric acid from Merck

(Darmstadt, Germany), and Tween20 from Carl Roth GmbH + Co (Karlsruhe, Germany).

Emulsion preparation

The emulsifiers—GGM, GX, and Tween20—were dissolved in 25 mM citrate buffer (pH 4.5) overnight at room temperature with magnetic stirring. By visual observation, the GGM and GX solutions were brownish and somewhat turbid. Rapeseed oil was added at an emulsifier : oil weight ratio of 1 : 5, and coarse oil-in-water emulsions with maximum 5 wt% emulsifier and 25% oil were prepared by homogenization with an Ultra-Turrax stirrer (T-18 basic, IKA, Staufen, Germany) at 9800 rpm for 5 min, followed by further homogenization with three passes through a high-pressure homogenizer at a pressure of 700 bar (Microfluidizer F20Y, Microfluidics, Westwood, MA, USA) to obtain fine emulsions. The homogenizer was configured with two 75 μm chambers in series. In addition, concentrated emulsions were prepared using 8% and 12% GGM and Tween20 and 40% and 60% oil by mixing using an Ultra-Turrax stirrer for 3–7 min at 10 000–18 000 rpm. The oil and emulsifier contents of the emulsions, as well as the preparation methods, are summarized in Table 1.

Droplet size

Droplet size distributions were obtained by using static light scattering (Horiba LA-950, Retsch Technology GmbH, Haan, Germany). The emulsions were dispersed in demineralized water and measured in triplicate. Refractive indexes of 1.333 for the water phase and 1.47 for the oil phase were used. Droplet size distributions were calculated according to the Mie theory. All measurements were performed using fresh emulsions. In addition, the droplet size distributions of GGM and GX emulsions were measured again after one month of storage at RT.

Interfacial tension

The interfacial tension of the continuous phases of the GGM5, GGM25, and GX25 emulsions, and that of the plain citrate buffer solution, were determined against rapeseed oil. A 15 μm droplet was squeezed to hang from the tip of a capillary in a cuvette filled with oil, and the droplet's shape was monitored for 2 h by using a KSV CAM 200 (Helsinki, Finland) contact angle and surface tension meter equipped with a camera and image analysis software. The surface tension of the solutions with higher GGM concentrations could not be measured owing to their high viscosity, and the measurement of Tween20 was unsuccessful because the Tween20 solution rapidly dispersed in oil.

ζ-Potential

To determine the ζ-potential, the GX5 emulsion was diluted 20 fold in de-ionized water and characterized in triplicate with a Zetasizer Nano ZS (Malvern Instruments Ltd).

Rheology

Rheological characterization of the emulsions and their constituents was performed at 25 °C by using an ARES-G2 strain-controlled rheometer (TA Instruments, 159 Lukens Drive, New Castle, DE 19720) having concentric cylinder geometry (r_1 = 18.6 mm and r_2 = 20 mm). Flow sweep measurements were performed over a range of 10–1300 l s^{-1}. Linear viscoelastic moduli were measured at a strain amplitude of 1%. Large-amplitude oscillatory shear flow measurements were performed at strain amplitudes between 30 and 700% at the angular frequencies ω = 1 and 20 rad s^{-1}. In addition to measurements on fresh emulsions, emulsion constituents, and cream, the analysis was repeated on all GGM emulsions and the GX25 emulsions after one month of storage at RT.

Conclusions

Wood hemicelluloses GGM and GX recovered from spruce and birch by the green and clean PHWE method efficiently enhanced the formation and stability of rapeseed oil-in-water emulsions with small droplet size. GGM are versatile stabilizers, showing emulsification and physical stabilization functions at a wide variety of oil volume fractions. Furthermore, GX, which have not been explored thus far, showed excellent emulsification and stabilization capacities. The rheological analysis revealed that GGM and GX show characteristics of steric emulsion stabilization. In comparison to the emulsions prepared with the classical small-molecular surfactant, Tween20, the use of GGM resulted in higher viscosity of the continuous phase, leading to enhanced emulsion stability against creaming. Depending on the oil volume fraction and droplet size, many of the GGM-containing emulsions remained stable over several months, while the Tween20-stabilized samples showed creaming after a few days. Owing to increased viscosity of the continuous phase, the GGM-stabilized emulsions retained their viscous behavior at high volume fractions, and yielding behavior, which is typical for highly concentrated emulsions, was not observed. These insights provide an understanding of and control over the processing and application conditions of emulsions stabilized using GGM and GX, novel wood-based hydrocolloids that could be exploited sustainably by various materials manufacturing industries in line with the future bioeconomy vision.

Abbreviations

GC	Gas chromatography
GGM	Galactoglucomannan
GX	Glucuronoxylan
HPSEC	High-performance size-exclusion chromatography
LAOS	Large amplitude oscillatory shear
PHWE	Pressurized hot water extraction
TMP	Thermomechanical pulping

Acknowledgements

We thank Mamata Bhattarai, Dr Leena Pitkänen, and Dr Mari Lehtonen for their assistance in the chemical characterization of GGM and GX and in interfacial tension measurements,

as well as Prof. Maija Tenkanen for fruitful discussions. We gratefully acknowledge The Academy of Finland (project No. 268144) and Nordic Forest Research (SNS, WOOD-PRO project) for funding.

References

1 L. L. Schramm, *Emulsions, Foams, Suspensions, and Aerosols*, Wiley-VCH, Weinheim, Germany, 2nd edn, 2014.
2 E. Dickinson, *J. Sci. Food Agric.*, 2013, **93**, 710.
3 K. S. Mikkonen, C. Xu, C. Berton-Carabin and K. Schroën, *Food Hydrocolloids*, 2016, **52**, 615.
4 M. Lehtonen, S. Teräslahti, C. Xu, M. P. Yadav, A.-M. Lampi and K. S. Mikkonen, *Food Hydrocolloids*, 2016, **58**, 255.
5 K. S. Mikkonen and M. Tenkanen, *Trends Food Sci. Technol.*, 2012, **28**, 90.
6 S. Willför, K. Sundberg, M. Tenkanen and B. Holmbom, *Carbohydr. Polym.*, 2008, **72**, 197.
7 P. Kilpeläinen, S. Hautala, O. Byman, J. Tanner, R. Korpinen, M. Lillandt, A. Pranovich, V. Kitunen, S. Willför and H. Ilvesniemi, *Green Chem.*, 2014, **16**, 3186.
8 T. Tadros, *Adv. Colloid Interface Sci.*, 2015, **222**, 692.
9 K. Reinheimer, M. Grosso and M. Wilhelm, *J. Colloid Interface Sci.*, 2011, **360**, 818.
10 P. Erni and A. Parker, *Langmuir*, 2012, **28**, 7757.
11 K. Hyun, M. Wilhelm, C. O. Klein, K. S. Cho, J. G. Nam, K. H. Ahn, S. J. Lee, R. H. Ewoldt and G. H. McKinley, *Prog. Polym. Sci.*, 2011, **36**, 1697.
12 K. Reinheimer, M. Grosso, F. Hetzel, J. Kübel and M. Wilhelm, *J. Colloid Interface Sci.*, 2012, **380**, 201.
13 C. Xu, S. Willför, K. Sundberg, C. Petterson and B. Holmbom, *Cellul. Chem. Technol.*, 2007, **41**, 51.
14 K. S. Mikkonen, M. Heikkilä, S. Willför and M. Tenkanen, *Int. J. Polym. Sci.*, 2012, 482810.
15 N. H. Maina, L. Pitkänen, S. Heikkinen, P. Tuomainen, L. Virkki and M. Tenkanen, *Carbohydr. Polym.*, 2014, **99**, 199.
16 P. Walstra, *Physical Chemistry of Foods*, Marcel Dekker, Inc., NY, 2003.
17 K. Parikka, A.-S. Leppänen, L. Pitkänen, M. Reunanen, S. Willför and M. Tenkanen, *J. Agric. Food Chem.*, 2010, **58**, 262–271.
18 C. C. Berton-Carabin and K. Schroën, *Annu. Rev. Food Sci. Technol.*, 2015, **6**, 263–297.
19 C. G. De Kruif, E. M. F. van Iersel, A. Vrij and W. B. Russel, *J. Chem. Phys.*, 1985, **83**(9), 4717–4725.
20 E. R. Morris, A. N. Cuttler, S. B. Roth-Murphy and D. A. Rees, *Carbohydr. Polym.*, 1981, **1**, 5–21.
21 C. Xu, S. Willför, P. Holmlund and B. Holmbom, *Carbohydr. Polym.*, 2009, **75**, 498.
22 E. Dickinson, M. I. Goller and D. J. Wedlock, *J. Colloid Interface Sci.*, 1995, **172**, 192–202.
23 Y. Saiki, C. A. Prestidge and R. G. Horn, *Colloids Surf., A*, 2007, **299**, 65–72.
24 Y. Otsubo and R. K. Prud'homme, *Rheol. Acta*, 1994, **33**, 29–37.
25 I. M. Krieger and T. J. Dougherty, *Trans. Soc. Rheol.*, 1959, **III**, 137–152.
26 J. Mewis and N. Wagner, *Colloidal Suspension Rheology*, Cambridge University Press, UK, 2012.
27 T. G. Mason, J. Bibette and D. A. Weitz, *J. Colloid Interface Sci.*, 1996, **179**, 439–448.
28 A. J. Giacomin and J. M. Dealy, in *Rheological Measurement*, ed. A. A. Collyer and D. Clegg, Chapman & Hall, 1998.
29 M. Wilhelm, *Macromol. Mater. Eng.*, 2002, **287**, 83–105.
30 R. Shu, W. Sun, T. Wang, C. Wang, X. Lio and Z. Tong, *Colloids Surf., A*, 2013, **434**, 220–228.
31 M. Hermes and P. S. Clegg, *Soft Matter*, 2013, **9**, 7568–7575.
32 R. Pal, *Food Hydrocolloids*, 2006, **20**, 997–1005.
33 H. M. Princen and A. D. Kiss, *J. Colloid Interface Sci.*, 1989, **128**, 176–187.
34 B. J. Maranzano and N. J. Wagner, *J. Chem. Phys.*, 2001, **114**, 10514–10527.
35 B. J. Maranzano and N. J. Wagner, *J. Rheol.*, 2001, **45**, 1205–1222.
36 R. G. Egres, F. Nettesheim and N. J. Wagner, *J. Rheol.*, 2006, **50**, 685–709.
37 B. Wolf, S. Lam, M. Kirkland and W. J. Firth, *J. Rheol.*, 2007, **51**, 465–478.
38 J. L. Leblanc, *Filled Polymers – Science and Industrial Applications*, CRC Press, Boca Raton, FL, 2010.
39 J. M. Brader, M. Siebenbürger, M. Ballauff, K. Reinheimer, M. Wilhelm, S. J. Frey, F. Weysser and M. Fuchs, *Phys. Rev. E: Stat., Nonlinear, Soft Matter Phys.*, 2010, **82**, 061401.
40 J. Kim, D. Merger, M. Wilhelm and M. E. Helgeson, *J. Rheol.*, 2014, **58**, 1359–1390.
41 F. Rouyer, S. Cohen-Addad, R. Höhler, P. Sollich and S. M. Fielding, *Eur. Phys. J. E: Soft Matter Biol. Phys.*, 2008, **27**, 309.
42 D. Merger, M. Abbasi, J. Merger, A. J. Giacomin, C. Saengow and M. Wilhelm, *Appl. Rheol.*, 2016, **26**, 53809, DOI: 10.3933/ApplRheol-26-53809.
43 N. Koumakis and G. Petekidis, *Soft Matter*, 2011, **7**, 2456–2470.
44 Z. Shao, A. S. Negi and C. O. Osuji, *Soft Matter*, 2013, **9**, 5492–5500.
45 T. Tadros, *Adv. Colloid Interface Sci.*, 2004, **108–109**, 227–258.
46 A. Ikeda, L. Berthier and P. Sollich, *Soft Matter*, 2013, **9**, 7669–7683.
47 L. Pitkänen, The effect of structure on the dilute solution properties of branched polysaccharides studied with SEC and AFFF, Doctoral thesis, University of Helsinki, Finland, 2011, available online at: http://urn.fi/URN:ISBN:978-952-10-7351-9.
48 A. Sundberg, K. Sundberg, C. Lillandt and B. Holmbom, *Nord. Pulp Pap. Res. J.*, 1996, **11**, 216–219, 226.
49 S.-L. Chong, S. Koutaniemi, L. Virkki, H. Pynnönen, P. Tuomainen and M. Tenkanen, *Carbohydr. Polym.*, 2013, **91**, 626.
50 L. Pitkänen, L. Virkki, M. Tenkanen and P. Tuomainen, *Biomacromolecules*, 2009, **10**, 1962.

